EMBRYONIC AND TISSUE-SPECIFIC REGULATION OF MYOSTATIN-1 AND -2 GENE EXPRESSION IN ZEBRAFISH

By

DERI LILA ICENOGGLE HELTERLINE

A thesis submitted in partial fulfillment of
the requirements for the degree of

MASTER OF SCIENCE

WASHINGTON STATE UNIVERSITY
Department of Animal Sciences

May 2006

To the Faculty of Washington State University:

The members of the Committee appointed to examine the thesis of DERI LILA ICENOGGLE HELTERLINE find it satisfactory and recommend that it be accepted.

_____
Chair

_____

_____

ACKNOWLEDGMENT

I would like to thank Dr. Buel D. Rodgers for the opportunity to work on a world-class project. I would like to acknowledge Dr. Deborah Stenkamp and Dr. Barrie Robison for supplying zebrafish and embryos, for without this support the project would not have succeeded. A sincere thank you to my entire committee for critically assessing my progress and helping me to become a better research scientist.

EMBRYONIC AND TISSUE-SPECIFIC REGULATION OF MYOSTATIN-1 AND -2 GENE EXPRESSION IN ZEBRAFISH

Abstract

By Deri Lila Icenoggle Helterline, M.S.
Washington State University
May 2006

Chair: Buel D. Rodgers

Myostatin is a member of the TGF-β superfamily and a potent negative regulator of muscle growth and development in mammals, where its expression is limited primarily to skeletal muscle. Conversely, myostatin expression occurs in many different fish tissues suggesting alternative functional roles in these vertebrates, although quantitative measurements of the embryonic and tissue-specific expression profiles in fish are lacking. A recent phylogenetic analysis of all known myostatin genes led to the discovery of a novel paralogue in zebrafish, zfMSTN-2, and the reclassification of the entire subfamily to include MSTN-1 and -2 sister clades in the boney fishes. The differential expression of both genes was therefore determined using custom RNA panels generated from pooled (100-150/sampling) embryos at different stages of development and from individual adult tissues. High levels of both transcripts were present at the blastula stage, but quickly dropped to almost undetectable levels throughout gastrulation (7 hpf). Levels of zfMSTN-2 peaked with an initial 5-fold increase during early somitogenesis (11 hpf), returned to basal levels during late somitogenesis and did not begin to rise again until hatching (72 hpf). By contrast, zfMSTN-1 mRNA levels increased 30-fold during late

somitogenesis (15.5-19 hpf) returned to baseline at 21.5 hpf and eventually rose 25-fold by 72 hpf. In adults, both transcripts were present in a wide variety of tissues. Although this distribution is similar to that previously described in zebrafish and other fish species, it includes additional tissues not previously known to express myostatin, including the spleen. Expression of zfMSTN-1 was highest in brain, muscle, heart and testes and was 1-3 log orders above that in other tissues. It was also greater than zfMSTN-2 expression in most tissues, nevertheless, levels of both transcripts increased 60-fold in spleens of fish subjected to stocking stress. These studies indicate that zfMSTN-1 and -2 gene expression is differentially regulated in developing embryos and in adult tissues. Their expression in spleens suggests the cytokines may additionally influence immune cell development. The increased expression of both genes in spleens from stressed fish is further supportive of an immunomodulatory role and may explain increased disease susceptibility associated with stocking stress.

TABLE OF CONTENTS

Page

LIST OF FIGURES

LIST OF TABLES

CHAPTER ONE

INTRODUCTION

Identifying Myostatin

Myostatin is a member of the TGF-β superfamily of growth and differentiation factors and was first identified by McPherron *et al.* in 1997. It is also a very potent negative regulator of mammalian skeletal muscle growth and development (McPherron and Lee, 1997). Several mammalian species have been shown to have extraordinary increases in skeletal muscle mass due to loss of function mutations in the myostatin gene. In a search for new members of the TGF-β superfamily, McPherron *et al.* (1997) screened known conserved regions of this family and obtained an unknown sequence, which was originally named GDF-8, and was found to be expressed specifically in developing and adult skeletal muscle of mice. However, GDF-8 was appropriately renamed myostatin when analysis of the gene revealed its biological activity. Whole mount *in situ* hybridization analysis during development of mice indicated that myostatin expression is restricted to the myotome compartment of developing somites. Further analysis detected myostatin in a wide range of developing adult skeletal muscles. In an analysis of 15 different adult tissues using northern blotting, myostatin was only expressed in skeletal muscle tissue. McPherron *et al.* (1997) then sought to determine the biological function of this new protein by creating myostatin knockout mice using a construct that targeted and deleted the entire C-terminal region. The resulting phenotype of the homozygous null mutants was incredibly enhanced musculature and body weights

that were 2-3 times greater than those of wild-type mice (Fig. 1). The greater musculature of the mutant mice was attributed to both increased hyperplasia, with nearly 86% higher cell number, and hypertrophy, with increase muscle fiber size between 14% and 49% above that of wild-type mice. A similar phenotype to the myostatin null mice has been described in several mammalian species including many domestic cattle breeds.

The heritable double-muscled phenotype in cattle was first documented nearly 200 years ago and has been most widely described in the Belgian Blue and Peidmontese breeds. Animals with this phenotype do not have an actual duplication of muscles, but this condition does involve both hyperplasia and hypertrophy of skeletal muscles (Arthur, 1995). Unlike mice however, myostatin null mutations in cattle causes an increase of only 20% to 25% in muscle mass. McPherron and Lee (1997) determined that the double-muscling phenotype in the Belgian Blue and Peidmontese breeds of cattle was attributed to mutations of the myostatin gene. To confirm that the double-muscle phenotype is due to mutations of the myostatin gene, all three exons of the Belgian Blue (BB) breed were amplified by PCR and subcloned. The sequence of the BB allele was identical to the Holstein breed except for a deletion of the nucleotides 937 through 947 in exon 3. This 11-nucleotide deletion causes a frame-shift mutation which results in a loss of 102 amino acids of the C-terminal region and is similar to the resulting knockout construct used to create the myostatin null mice (Grobet et al., 1997; McPherron and Lee, 1997). Although the Piedmontese breed double-muscle phenotype is comparable to that of Belgian Blue cattle, the mutation in the myostatin gene is different. The Piedmontese sequence contains a guanine to adenine transition in exon 3, resulting in a cysteine to tyrosine substitution in the bioactive domain of the protein. This particular residue is critically

important to the formation of a disulfide linkage that helps form a "cystein knot". A second mutation was also detected, cytosine to adenine transition in exon 1 that results in a relatively conserved substitution of leucine for phenylalanine, although this is not suspected to influence myostatin function (Grobet et al., 1997; Kambadur et al., 1997; McPherron and Lee, 1997). In both breeds of cattle, mutations of the myostatin gene were found to occur on both alleles. A splice-site mutation (exon 1) was recently described in a human baby boy with dramatically enhanced musculature, so much so, that at birth the child had protruding muscles in his thighs (Schuelke et al., 2004). The child has developed normally except for his above normal strength, and at 4.5 years of age he was able to hold two 3-kg dumbbells in horizontal suspension with his arms extended. Therefore, it is apparent that disrupting myostatin production in mammals stimulates muscle growth and development that results from increases in both the number of muscle fibers as well as fiber size (Fig 1.) (Lee, 2004).

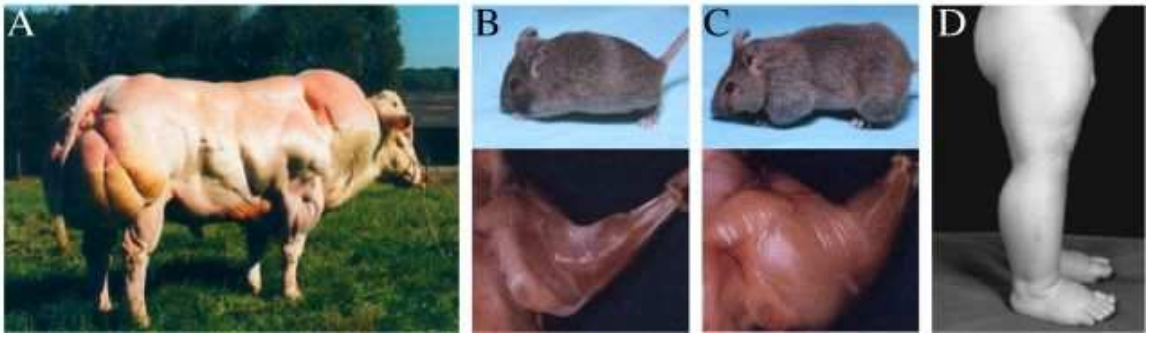

Figure 1. "Double-muscling" in myostatin-null animals. (A) Double-muscling in Belgian Blue cattle breeds (published by McPherron et al., Nature 387:83-90, 1997). Forearm musculature of wild-type (B) and myostatin knock-out mice (C) (published by McPherron and Lee Proc. *Natl. Acad. Sci.* 94:12457-12461, 1997. (D) Leg musculature of 7-month old infant with myostatin mutation (published by Schuelke et al. *N. Engl. J. Med* 350:2682-2688, 2004).

Protein processing, dominant-negative interference & receptor activation.

The primary translated product from myostatin mRNA is eventually processed into two distinct dimeric peptides: the latency associated protein (LAP, a.k.a. "prodomain") and the bioactive peptide, myostatin (Fig. 2). Like other members of the TGF-β superfamily, both LAP and myostatin are believed to be secreted together where they associate as a "small latent complex" with the extracellular matrix and as yet an unidentified binding protein (Saharinen et al., 1999). Assuming the TGF-β model for activation is conserved with myostatin, proteolysis of the complex releases myostatin, which is then free to activate relevant receptors including those for activin. Lee and McPherron (Lee and McPherron, 2001a) overexpressed different receptors for known TGF-β superfamily ligands in COS-7 cells and demonstrated that [^{125}I]-murine myostatin crosslinked to activin type I and II B receptors (ActRIB & ActRIIB), although the association with ActRIIB was significantly more pronounced. Scatchard analysis with COS-7/ActRIIB cells indicated that binding was saturable, specific and had a dissociation constant of approximately 10 nM. In addition, [^{125}I]-myostatin binding was displaced by follistatin, an activin binding protein, or by LAP. These displacement interactions were direct as both follistatin and LAP sequestered myostatin away from its receptor. The authors additionally constructed transgenic mice that separately overexpressed each interfering peptide or a dominant-negative ActRIIB, producing "double muscled" phenotypes that were similar to myostatin knockout mice. Zimmers *et al*. (Zimmers et al., 2002) similarly showed that follistatin blocks myostatin activity *in vitro* and *in vivo* by the implantation of CHO cell tumors overexpressing the follistatin peptide in nude mice. These studies suggest that in mammals, the anti-myogenic actions of myostatin are

mediated in large part by activin receptors and that mechanisms meant to block ActRIIB activation (i.e. LAP or follistatin binding) interfere with the actions of myostatin.

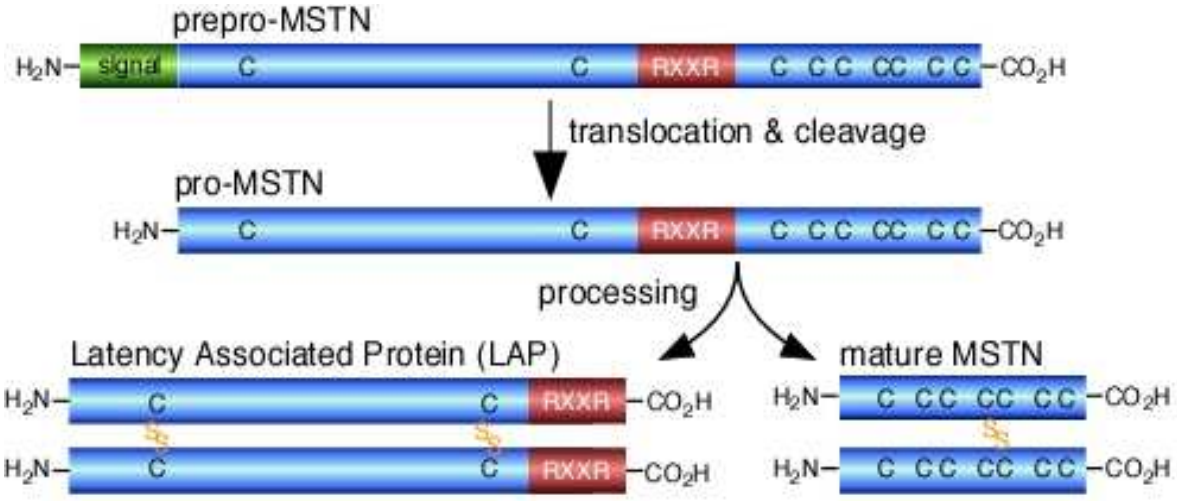

Figure2. Proteolytic processing of myostatin (MSTN). Pro-MSTN is cleaved at a conserved RXXR epitope and the resulting peptides for disulfide-linked homodimers. Dominant-negative forms consist of LAP dimers alone, which sequester endogenously produced bioactive MSTN dimers.

Regulation of growth and differentiation by myostatin

Developing vertebrate skeletal muscle originates from the somatic mesoderm, specifically the paraxial mesoderm, which is the precursor to the somites. The presumptive myoblasts within the myotome compartment of each somite eventually migrate to the periphery where they ultimately undergo a terminal mitotic division to become postmitotic myoblasts, most of which fuse to form myotubes. In turn, the fully differentiated myotubes begin to synthesize the principal contractile proteins that eventually form mature muscle fibers. This process is controlled intracellularly by the basic helix-loop-helix family of transcription factors known as the myogenic regulatory factors (MRFs). In fact, the most influential member of this family, MyoD, is capable of initiating myogenesis alone even in some non-muscle cells (Molkentin and Olson, 1996; Rudnicki and Jaenisch, 1995). As a group, the MRFs are expressed in sequential order (Myf-5, MyoD, myogenin & MRF4), which helps to mediate the two principal processes involved in skeletal muscle development: myogenic determination and myoblast differentiation (Megeney and Rudnicki, 1995; Valdez et al., 2000). Expression of the primary MRFs, Myf-5 and MyoD, occurs before the onset of myoblast differentiation and helps commit somite or satellite cells to the myogenic lineage, whereas expression of the secondary MRFs, myogenin and MRF4, occurs well after determination and is responsible for the terminal differentiation and maturation of skeletal muscle cells (Arnold and Braun, 1996; Rudnicki and Jaenisch, 1995).

The multifactoral regulation of MRF gene expression and skeletal muscle development in general is orchestrated extracellularly by many different growth factors and cytokines, including the insulin-like growth factors (IGF-I & -II) and myostatin. The

IGFs stimulate myoblast differentiation by modulating the intracellular levels and activity of cyklin-dependent kinases (Cdk's) and other downstream effectors. They are also potent mitogens capable of stimulating myoblast proliferation via MAP kinase-dependent pathways (Zapf and Froesch, 1999). This obscure ability to stimulate both processes involved in muscle development is dependent upon cell cycle progression for myoblast proliferation and growth arrest for differentiation; two opposing processes that in general are inversely regulated. In contrast to the dual stimulatory effects of IGF-I, myostatin suppresses both myoblast proliferation and differentiation (Langley et al., 2002; Rios et al., 2001b; Taylor et al., 2001; Thomas et al., 2000b).

Cyclin dependent kinase complexes play important roles in the G_1 to S-phase progression of the cell cycle through phosphorylation of the retinoblastoma protein (Rb). Inhibitors of these complexes include members of the p16 and p21 families. Thomas *et al*. (2000) treated C_2C_{12} myoblasts with myostatin and reported an up-regulation of p21 levels while Cdk2 levels and activity decreased. Myostatin's inhibition of myoblast proliferation is thus mediated by activating and increasing levels of the Cdk2 inhibitor p21, while rendering the Cyclin-E•Cdk2 complex inactive. This in turn results in the suppression of Rb phosphorylation and arrests myoblasts in the G_1 phase of the cell cycle (Lee, 2004; Rios et al., 2001a; Thomas et al., 2000a). Treatment of C_2C_{12} myoblasts and primary bovine myoblasts with myostatin also inhibits myoblast differentiation (Langley et al., 2002), which appears contradictory since cell cycle arrest is required for differentiation. Interestingly, when myostatin was removed from the media, myoblasts were able to continue with the differentiation process, indicating that myostatin inhibition of differentiation is reversible and that myostatin maintains cells in a quiescent state.

These inhibitory actions are mediated though the down-regulation of MyoD, myogenin and Myf5, which blocks both muscle cell determination as well as maturation (Joulia et al., 2003; Langley et al., 2002; Rios et al., 2002).

Expression analysis of myostatin

Analysis of myostatin gene expression in mammals indicates that it plays an important role in the regulation of developing muscle. In embryos, myostatin expression is first detected in the myotome compartment of developing somites, its expression continues in developing skeletal muscle and is limited primarily to this tissue in adults, however weak expression has also been detected in Purkinje fibers and cardiomyocytes of sheep (Sharma et al., 1999), in porcine lactating mammary glands (Ji et al., 1998) and in adipose tissue (McPherron and Lee, 2002). Myostatin expression has also been determined in several fish species and was first described in tilapia and white bass (Rodgers et al., 2001a). Since the initial discovery, several additional cDNA clones have been characterized from different commercially important species including striped bass and white perch (Rodgers and Weber, 2001), brook trout, yellow perch, mahi-mahi, little tunny and king mackerel (Roberts and Goetz, 2001), Atlantic salmon (Ostbye et al., 2001), rainbow trout (Rescan et al., 2001), channel catfish (Kocabas et al., 2002) and zebrafish (Ken et al., 2000; Vianello et al., 2003; Xu et al., 2003). Qualitative measurements indicate that fish express the myostatin gene in a wide variety of tissues in addition to skeletal muscle including brain, eyes and gonads (Maccatrozzo et al., 2001a; Maccatrozzo et al., 2001b; Radaelli et al., 2003; Rescan et al., 2001; Roberts and Goetz, 2001; Rodgers and Weber, 2001; Rodgers et al., 2001a). Conversely, mammals express myostatin predominately in skeletal muscle (Lee and McPherron, 1999). This contrasting

expression pattern in fish versus mammals suggests divergent mechanisms of gene expression, regulation and in particular alternative functions that extend well beyond muscle growth inhibition.

The myostatin protein is highly conserved among vertebrate species, particularly in the bioactive domain, suggesting conservation among functions (Rodgers and Weber, 2001). However, a recent phylogenetic analysis performed in our laboratory identified a novel myostatin gene in zebrafish and indicated that all fish possess at least two myostatin genes: MSTN-1 and -2 (Kerr et al., 2005). This study also reclassified the entire TGF-β subfamily to include MSTN-1 and -2 sister clades in the boney fishes. This study also suggests that previous expression studies in fish are somewhat ambiguous as they were either measuring MSTN-1 or both transcripts simultaneously. Thus, these assessments of myostatin gene expression in fish are misleading, and may not be entirely reliable as they are complicated by the potential presence of multiple gene products.

Correlation between stress and myostatin

The role of myostatin in any animal has yet to be fully determined, however stress and illness may be indicators of the differential regulation of myostatin between fish and mammals. In teleosts, stress activates the hypothalamus-pituitary-interrenal (HPI) axis, leading to the release of adrenocorticotropic hormone (ACTH) from the anterior pituitary gland, which then stimulates the synthesis of glucocorticoids from the interrenals (Bern, 1992; Mommsen, 1999; Wendelaar Bonga, 1997). The glucocorticoid cortisol enters target cells by passive diffusion and once inside the cell it binds to high affinity cytosolic receptors, which acts as a ligand dependent transcription factor to control gene expression (Evans, 1988). Stress induced release of glucocorticoids may be one of many factors that

influence skeletal muscle condition and myostatin production. In humans, serum levels of myostatin are elevated in HIV-infected individuals with muscle wasting (Gonzalez-Cadavid and Bhasin, 2004). Myostatin protein levels are also elevated in rat muscle during hindlimb unloading and in response to heat stress (Baldwin, 1996). This latter effect is due to direct stimulatory actions of glucocorticoids on myostatin gene expression. By contrast, chronic stocking stress decreases myostatin levels in zebrafish skeletal muscle (Vianello et al., 2003), as does chronic nutritional stress in larvae of another fish species, tilapia (Rodgers et al., 2003). The relationship between stress and myostatin production in any tissue other than muscle has not yet been studied and is particularly important in fish where myostatin expression occurs in many different tissues.

Justification of myostatin expression analysis

As in mammals (McPherron et al., 1997), myostatin expression is developmentally regulated in zebrafish and in other fish species as well (Rodgers et al., 2001b; Vianello et al., 2003; Xu et al., 2003). Proteolytic processing and secretion of myostatin is also conserved and has been confirmed *in vivo* (Rodgers and Weber, 2001) and *in vitro* (Roberts and Goetz, 2003; Vianello et al., 2003). Maternal transcripts can be detected in unfertilized eggs and in early embryonic stages but are undetected during gastrulation and rise consequentially after eyeing. In fact, changes in its expression during larval development correspond well with the emergence of skeletal muscle (Rodgers et al., 2001a). These studies however may be misleading as the transcripts analyzed may have been either MSTN-1 or both MSTN-1 and -2 together. Xu *et al.* (Xu et al., 2003) demonstrated that although MSTN-1 mRNA could be detected by RT-PCR

in zebrafish embryos, transcript levels were too low to be detected by *in situ* hybridization, which was also true for MSTN-2 (Kerr et al., 2005). The developmental expression pattern *in vivo* was therefore determined using transgenic fish transiently expressing a GFP reporter gene under the direction of 1.2 kb of the zebrafish myostatin promoter. Although GFP expression occurred in mature myofibers, it was additionally detected in the forebrain and floor plate, but was not detected in the somites. Furthermore, muscle-specific expression of the zebrafish LAP produced only minor changes in hyperplastic muscle growth (12% increase in fast muscle of females only and no change in slow muscle or in fiber diameter), which was considerably different from the double-muscled phenotype of LAP transgenic mice (Lee and McPherron, 2001b). They also determined that mRNA levels of different MRFs were unaffected by overexpressing LAP using quantitative real-time PCR. Some of these studies were recently repeated by Amali *et al*. (Amali et al., 2004) who, using *in situ* hybridization, reported ubiquitous expression of myostatin in virtually every tissue throughout embryonic development. These results are somewhat controversial as the sense strand controls were never shown and because they are in stark contrast to Xu *et al*. (2003) and to previous studies with mice (McPherron et al., 1997). Using antisense morpholinos, Amali *et al*. (2004) purported to have also disrupted embryonic myostatin expression, which appeared to have multiple effects on somitogenesis and on whole embryo size. Levels of MyoD and myogenin mRNA were also reported to have increased with morpholino treatment, although this was assessed using non-quantitative PCR methods. Attempts to validate the efficiency of morpholino "knock-down" by western blotting for myostatin protein using anti-human myostatin antiserum identified a single band of 27

kDa under reducing and denaturing conditions. This again is in stark contrast to Vianello *et al*. (Vianello et al., 2003) who identified the expected 13 kDa processed and 42 kDa unprocessed myostatin proteins using two different antisera generated specifically against zebrafish myostatin. Therefore, it is difficult to determine whether morpholino treatment of embryos had any specific effects on myostatin production and thus, on embryonic development and MRF expression.

Given that previous studies of myostatin gene expression during the development of fish did not differentiate between MSTN-1 and -2 genes, and that nearly all of the studies were only qualitative assessments, we sought to determine expression patterns of zfMSTN-1 and -2 genes and to quantify the relative amounts of each transcript in developing zebrafish embryos and in different adult tissues. We hypothesized that although both genes may be similarly expressed, unique patterns will emerge and that the relative degree of expression may be quite different between genes. Our results indicate that zfMSTN-1 and -2 are indeed differentially regulated in developing embryos and in adult tissues. These studies additionally suggest that zfMSTN-1 and -2 may also have immunomodulatory roles in fish that may contribute to stress-induced immunocomprimization.

CHAPTER TWO

EMBRYONIC AND TISSUE-SPECIFIC REGULATION OF MYOSTATIN-1 AND -2 GENE EXPRESSION IN ZEBRAFISH

Introduction

As discussed earlier, myostatin is a member of the TGF-β superfamily of growth and differentiation factors, known mostly for its potent negative regulation of mammalian skeletal muscle. In fish, however its function may be more diverse and may influence many other tissues. Recent studies demonstrate that it is expressed in a wide variety of tissues, unlike mammals where it is expressed primarily in skeletal muscle. Zebrafish myostatin was the first identified non-mammalian homologue to be sequenced in (McPherron et al., 1997) and since then the expression of different homologs have been identified in various tissues of different fish species (Table 1). Myostatin protein also appears to be widely distributed as myostatin immunoreactivity was identified in several tissues of juvenile and larval zebrafish, sole and seabream (Radaelli et al., 2003)

To date, most analyses of myostatin expression in developing and adult fish have been qualitative. Attempts to determine expression patterns with *in situ* hybridization have failed because the level of myostatin expression is too low to be detected by this method (Vianello et al., 2003; Xu et al., 2003). All other analyses have used RT-PCR to determine expression of myostatin. In tilapia, myostatin was first detected in post-hatching larvae, however it was not detected in fertilized oocytes or in prehatching larvae with eye spots (Rodgers et al., 2001a). Myostatin expression was first detected in catfish embyros beginning at 1 day post-fertilization, but this expression required 35 cycles of

PCR and was relatively weak. RT-PCR analysis of myostatin expression in zebrafish detected the mRNA in just-fertilized embryos, which is consistent with maternally transcribed transcript (Vianello et al., 2003). The transcript appeared to decrease during gastrulation, and increase slightly during mid-somiteogenesis, then steadily rise throughout development until adulthood. Xu *et al*. (2003) was able to detect myostatin from 1-4 days post-fertilization. While these studies are able to detect myostatin in developing fish, none specifically address expression during somitogenesis, when myogenesis occurs, nor do they attempt to quantify expression during this most significant stage of muscle development. These studies were also conducted before the recent discovery of the MSTN-2 subfamily and may be unreliable due to complications associated with primer/probe specificity (Kerr et al., 2005).

Given that previous studies of myostatin gene expression during the development of fish did not differentiate between MSTN-1 and -2 genes, and that nearly all of the studies were only qualitative assessments, we sought to determine the expression patterns of zfMSTN-1 and -2 genes and to quantify the relative amounts of each transcript in developing zebrafish embryos and in different adult tissues. We hypothesized that although both genes may be similarly expressed, unique patterns will emerge and that the relative degree of expression may be quite different between genes. Our results indicate that zfMSTN-1 and -2 are indeed differentially regulated in developing embryos and in adult tissues. These studies additionally suggest that zfMSTN-1 and -2 may also have immunomodulatory roles in fish that may contribute to stress-induced immunocomprimization.

Table 1. Myostatin expression of mRNA in fish tissues.

Tissue	*tilapia*[1]	*seabream*[2]	*brook trout*[3]	*rainbow trout*[4]	*channel catfish*[5]	*Atlantic salmon*[6]
Brain	+		+	+	+	+
Skeletal muscle	+	+	+	+	+	+
Gill	+			+	+	+
Eye	+	+			+	+
Skin						
Gastrointestinal tract	+	+		+	+	+
Heart		+		+	+	
Spleen					+	+
Liver				+	+	
Swim bladder					+	
Kidney		+		+	+	
Ovaries	+	+	+	+		+
Testes	+			+		+
Adipose						

[1.] Rodgers et al. (2001); [2.] Maccatrozzo et al. (2001b); [3.] Roberts and Goetz (2003); [4.] Rescan et al. (2001); [5.] Kocabas et al. (2002); [6.] Ostbye et al. (2001)

Materials and Methods

Animal Studies

The zebrafish *Danio rerio* used in this study were housed in a centralized facility at the University of Idaho. All experiments were performed in accordance with the Animal Care and Use Committees of the University of Idaho and Washington State University under preapproved protocols. Fertilized eggs of the Scientific Hatcheries wild-type strain were collected from several broodstock induced to spawn naturally under temperature and photoperiod control. Eggs were fertilized at dawn and collected within 30 minutes. Embyos were collected according to developmental stages as referenced in The Zebrafish Book (2000). Developmental stages of collection were mid-blastula (4 hours post-fertilization, hpf), mid-gastrula (7 hpf), several stages of somitogenesis (4 somites - 11.3 hpf , 8 - 13, 13 - 15.5, 17 - 17.5, 20 - 19, 25 -21.5 , 24, 48 and 72 hpf). Samples were also obtained from adult zebrafish after euthaniztion with a lethal dose of tricane methansulfonate (MS222, Argent, argent-labs.com). Individual tissues including brain, skeletal muscle, gill, eye, skin, gastrointestinal tract, heart, spleen, liver, swim bladder and gonads of both sexes were dissected and snap frozen in liquid nitrogen.

Quantitative expression analysis of myostatin-1 and -2 using RT-PCR

Total RNA was extracted from *Danio rerio* embryos (100-150 embryos per development stage) and adult tissues with TRIzol (Invitrogen, invitrogen.com) reagent according to the manufacturer's instructions. cDNA was synthsized using the First Strand cDNA synthesis kit (Invitrogen). A qualitative analysis of zfMSTN-1 and -2 mRNA levels was performed by reverse transcriptase (RT-PCR). However, a quantitative real-time RT-PCR assay (see below) was also performed, although the same gene specific

primers were used in the same assays. For each primer pair, the forward primer targeted the coding region in exon 1 and the reverse primer in exon 2 (Kerr et al., 2005; Xu et al., 2003), thus amplicons from both primer sets spanned the first intron of each respective gene. The sequence for the zfMSTN-1 forward primer was 5'-ACA TGC CAC CAC AGA AAC CA -3' and the reverse was 5'-CAA CAC TTC GGT TTC CGA TCT AC-3'. The forward zfMSTN-2 primer was 5'-GCA AGC AGC GAG ACC ATC AT-3' and the reverse was 5'-CAT GCA ACA CTT CGG CAT TC-3'. Expression of elongation factor 1-α (EF1-α) was monitored and was used as a reference control. Its forward primer sequence was 5'-GCA TAC ATC AAG AAG ATC GGC -3' and its reverse primer was 5'-GCA GCC TTC TGT GCA GAC TT G-3'. A mastermix with cDNA was created before aliquoting and before the addition of gene specific primers. After an initial denaturation at 94°C for 4 min and 72°C for 1 min samples were then amplified for 40 cycles (30 sec at 94°C, 15 sec at 58°C and 1 min at 72°C) with a final elongation step of 5 min at 72°C. Each sample volume was in a 50 µl which contained 0.2 µM of each primer and was comprised of commercial reagents (Invitrogen)

Real-time PCR analysis of myostatin gene expression

Real-time RT-PCR was performed using the same primers as described for RT-PCR using the iCyler IQ real time PCR detection system (Biorad, bio-rad.com). Samples were amplified for 45 cycles (95°C for 30 sec, 58°C for 30 sec and 72°C for 30 sec) using primer concentrations that were empherically determined. A melt curve analysis preformed with each reaction was used to determine if gDNA contamination was present. Each sample aliquot of 25 µl for zfMSNT-1 and zfMSTN-2 contained 5 µl cDNA, for EF1-α reactions only 1.5 µl cDNA was used. zfMSTN-1 forward primer concentration

was 72 nM, reverse primer concentration was 48 nM, zfMSTN-2 forward and reverse primer concentrations were both used at 72 nM, EF1-α forward primer concentration was 48 nM and reverse primer concentration was 72 nM. IQ SYBR Green was included in the PCR reaction as described in the protocol of IQ SYBR Green PCR (Biorad). For each timepoint, samples were run in triplicate on each plate and each analysis was repeated. Three control wells were also included on each plate that consisted of a no template control (NTC) and a RT- (RNA only) control.

Stocking density stress and myostatin expression

Two stocking densities of adult Scientific Hatcheries zebrafish were used to measure zfMSTN-1 and -2 gene expression in individual tissues and included high (HD) and low (LD) density groups that were housed in identical environments. The HD or "stressed" fish were housed at a density of 40 fish/L (32g/l fish) and the LD control fish were housed using a density of 5 fish/L (4g/L). Three tanks housed fish at either density for a total of 6 tanks, to control for tank effect, and the experiment was repeated. Fish were watched when fed to ensure satiety was reached and there were no deaths or illnesses observed during these experiments. All 5 fish from each of the LD tanks and 5 fish from each of the HD tanks were euthanized after first submersing in a lethal dose of tricane methansulfonate (MS222). The remaining fish from the HD tanks were returned to the general population. Brain, skeletal muscle and spleen were dissected from the euthanized fish and processed as described above

.

Statistical analysis

The threshold cycle (Ct) was calculated for each quantitative "real-time" RT-PCR sample run and expression levels were calculated using *Q-Gene* software (Muller et al., 2002) according to the formula for the calculation of the Normalized Gene Expression,

$$NE = \frac{(E_{ref})^{CT_{ref}}}{(E_{t\arg et})^{CT_{t\arg et}}}$$ (normalized expression, NE; target amplification efficiency, E_{target}; reference gene amplification efficiency, E_{ref}; threshold cycle target gene, CT_{target}; reference threshold cycle, CT_{ref}) The Ct is defined as the cycle at which fluorescence rises appreciably above the background fluorescence. The mean normalized expression was calculated by averaging three independently calculated normalized expression values of the triplicate and repeat. Standard error of the mean values were calculated using the formula for the calculation of the Standard Error of the Mean Normalized Gene Expression

$$\Delta MNE = \frac{(E_{ref})^{CT_{ref}}}{(E_{t\arg et})^{CT_{t\arg et}}} \bullet \sqrt{(\ln(E_{ref}) \bullet \Delta CT_{ref,mean})^2 + (\ln(E_{t\arg et}) \bullet \Delta CT_{t\arg et,mean})^2}$$

(standard error of the mean normalized expression, ΔMNE; mean threshold cycle of the target gene, $CT_{target,mean}$; mean reference gene amplification efficiency, $CT_{ref,mean}$; standard error of the mean the target gene amplification efficiency, $\Delta CT_{target,mean}$; standard error of the mean reference gene amplification efficiency, $\Delta CT_{ref,mean}$). Differences between means (+/- SEM; n=15) were determined by a *t*-test ($p \leq 0.05$)

Primer design for real-time RT-PCR

The most important first step when using real-time RT-PCR is to design primers properly. The following guidelines specifically refer to SYBR green I assays. As SYBR

green I binds to any dsDNA it is important to avoid primer-dimer and/or non-specific products. By selecting amplicons between 80 and 150 base pairs, a high level of fluorescence can be obtained without compromising PCR efficiency.

Computer software such as PrimerExpress® is very helpful in designing high quality primers. When designing primers, be sure that the following parameters are followed. Each primer should be between 18 and 30 bases in length. The G to C content should be within the range of 30% to 80%, but ideally within 40% to 60%. The melting temperature (Tm) should be within the range of 63°C to 67°C, ideally 64°C, so that the annealing temperature is between 58°C and 62°C. The difference in Tm between primers should be less than 4°C. Design intron spanning primers to prevent or identify the amplification of contaminating gDNA. For intron spanning primers, the first half of the oligo must hybridize with the 3' end of one exon and to the 5' end of the other exon. In this way, only cDNA will be amplified and not gDNA. Amplicons generated from cDNA, without introns, will be smaller than amplicons from gDNA. The difference in size of these amplicons can be determined by melt curve analysis and by agarose gel electrophoresis. Genomic DNA is best avoided by DNase treatment of the RNA with RNase free DNase.

The following are things to avoid when designing primers. Mismatches between primers and target, especially at the 3' end of the primer, can occur if there are multiple T's at the 3' end or if there are runs of identical nucleotides, especially 3 or more G's or C's . To reduce hairpins and primer-dimer, avoid complementarity especially at the 3' end.

Results

Primer validation. The high conservation of the zfMSTN-1 and -2 genes complicate PCR-based analyses of individual transcript levels. Therefore gene-specific primers were carefully designed and validated using a primer mismatch assay that paired zfMSTN-1 primers with zfMSTN-2 cDNA plasmids and *vice versa*. A temperature titration assay was also performed for each primer to determine the safe maximum range of annealing temperatures that would avoid primer cross-hybridization. For both zfMSTN-1 and -2 primer temperature sets, ranged from 50°C to 65°C, while the temperature range for the reference gene (EF1-α) was 52°C to 59°C (Fig. 3A). All primers successfully amplified appropriate template even at the highest temperatures tested, which were 3-8°C above the respective calculated Tm. Using these annealing temperatures, both primers were proven valid as they only amplified their specific targets.

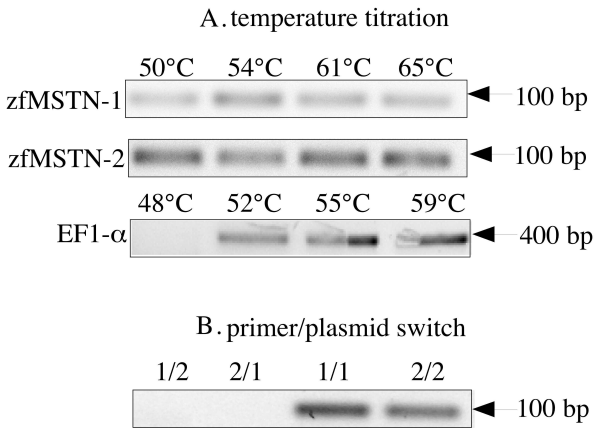

Figure 3. Primer validation. A. Primers for zfMSTN-1, -2, and EF1-α were used to amplify adult zebrafish skeletal muscle cDNA using the annealing temperatures indicated. B. Assessment of potential primer cross-reactivity. Plasmids containing cDNA for each myostatin were amplified with specific or non-specific primers (1/2 = zfMSTN-1 plasmid + zfMSTN-2 primers, etc.).

Qualitative and quantitative assessment of zfMSTN-1 and -2 developmental expression. Using the former assay, levels of the zfMSTN-1 and -2 transcripts were initially assessed by normal RT-PCR and later by real-time RT-PCR. The expression patterns and levels of both transcripts were determined using pooled samples of 100-150 embryos per stage of development, which thereby diluted individual variation. The transcripts were weakly expressed throughout development, although zfMSTN-1 levels were more readily detected at each timepoint (Fig 4.) Nevertheless, differences between different stages could not be resolved as expression levels were at the limit of detection. This was apparently was not due to poor sample quality as RNA fidelity was verified by gel electrophoresis and because EF1-α was easily amplified in all samples. Rather than optimizing this assay for semi-quantitative results only, we assayed the same samples using quantitative real-time RT-PCR assay.

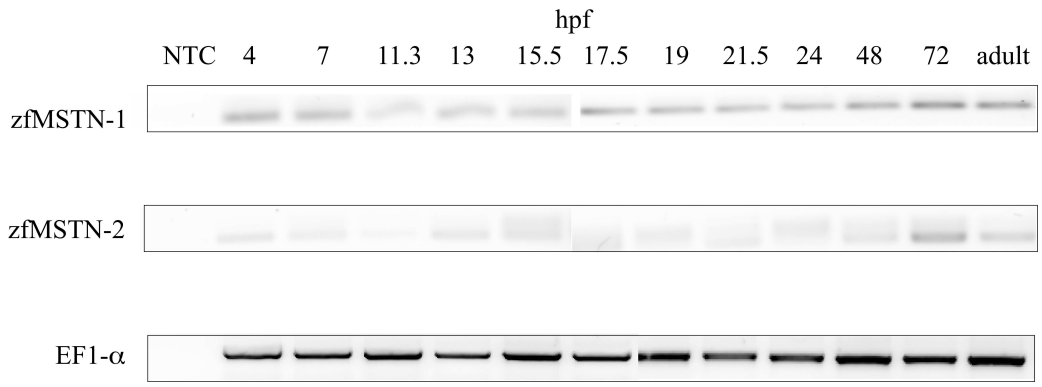

Figure 4. Qualitative assessement of zfMSTN-1, -2, and EF1-α expression throughout embryogenesis. Levels of each transcript were qualitatively assessed by RT-PCR using embryos collected at the indicated time (hpf, hours post-fertilization). Adult RNA was extracted from skeletal muscle. (NTC, no template control; 11.3 hpf, 4 somite; 13, 8 somite; 15.5, 13 somite; 17.5, 17 somite; 19, 20 somite; 21.5, 25 somite).

High levels of both zfMSTN-1 and -2 transcripts were present at the blastula stage (4 hpf), but quickly dropped to almost undetectable levels throughout gastrulation (7 hpf). The presence of both transcripts during the blastula stage is likely attributed to the transfer and of maternal. Both transcript levels increased steadily following somitogenesis, although the rate and absolute degree increase in zfMSTN-1 levels were substantially greater than those of zfMSTN-2. Indeed zfMSTN-1 levels were always greater than those of zfMSTN-2 and were approximately 28-fold greater than at the end of somitogenesis (Fig 5A). A closer evaluation of the gene expression patterns during somitogenesis reveals a zfMSTN-2 peak due to with an initial 5-fold increase during early somitogenesis (11.3 hpf) (Fig 5B). Expression returned to basal levels during late somitogenesis and did not begin to rise again until hatching (72 hpf), which continued into adulthood (data not shown). By contrast, zfMSTN-1 mRNA levels were low during early somitogenesis (11.3-13 hpf), but increased 30-fold during late somitogenesis (15.5-19 hpf) before returning to basal levels at the end of this developmental period (21.5 hpf). These data indicate that zfMSTN-1 and -2 gene expression is differentially regulated in developing embryos. Specifically during early and late somitogenesis and during the events that preclude hatching.

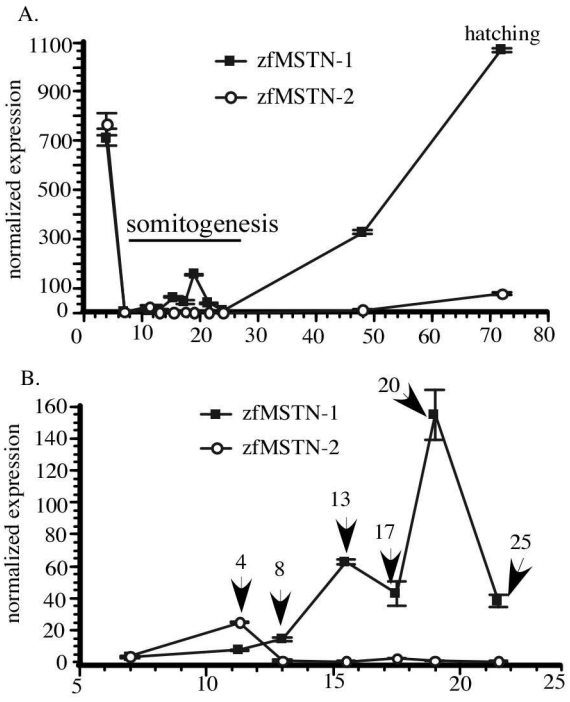

Figure 5. Quantitative analysis of zfMSTN-1 and -2 mRNA levels in developing embryos. A comprehensive RNA panel was constructed by staging and individually sampling 100-150 embryos at the time periods indicated (4, 7, 11.3, 15.5, 17.5, 19, 21.5, 24, 48 and 72 hpf). A. Transcript levels of both zfMSTN-1 and -2 were measured using real-time RT-PCR and were normalized to those of EF1-α. B. Transcript levels during early development. Arrows indicate somite number. Mean values are shown (+/- SEM) for each timepoint.

In previous studies, myostatin has been found to be expressed in many different fish tissues however, these analysis only studied zfMSTN-1 expression patterns or both transcripts simultaneously. Therefore total RNA was isolated from twelve tissues of zebrafish adults and was analyzed by quantitative real-time RT-PCR to determine individual tissue expression patterns of zfMSTN-1 and -2. In adults, both transcripts were present in brain, muscle, gill, eyes, skin, gastrointestinal tract, heart, spleen, liver, swim bladder and gonads of both sexes. This distribution includes tissues not previously known to express myostatin, including liver, heart and spleen. Normalized expression of zfMSTN-1 was highest in brain, muscle, heart and testes and was 1-3 log orders above that in other tissues, it was lowest in swim bladder and liver. It was greater than zfMSTN-2 expression in all tissues except eyes and swim bladder. Normalized expression zfMSTN-2 transcript was greatest in brain, eyes, spleen and testes and was 1-4 log orders above that of other tissues, it was lowest in gills and gastrointestinal tract (Fig. 6). These studies suggest alternative functional roles for zfMSTN-1 and -2 during embryogenesis and in adult tissues. Previously, the functional role of myostatin was thought to be restricted to skeletal muscle, however levels of expression of both genes in spleen and other tissues raises the possibility of immunomodulatory functions.

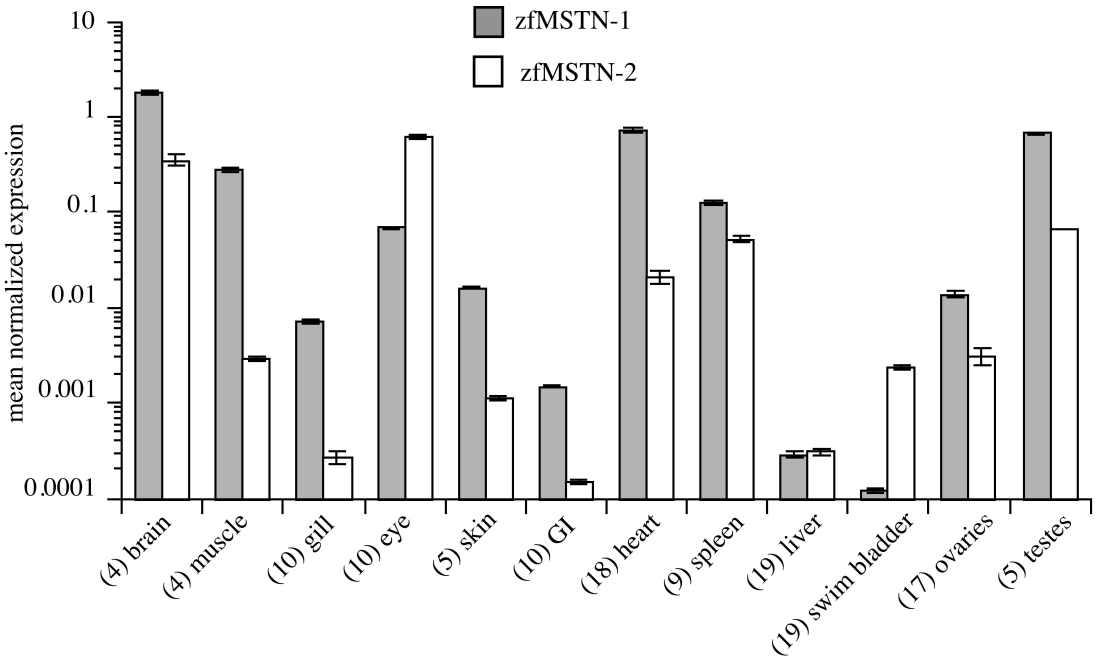

Figure 6. Adult tissue distribution of zfMSTN-1 and -2 mRNA. Total RNA was isolated from tissues of adult zebrafish and analyzed using qRT-PCR. Transcript levels were normalized to EF1-α. Assays were repeated in triplicate and tissues were sampled twice (representative assay shown). Mean values are shown for each tissue, which represents a pooled sampling from several animals (numbers indicated). Error bars (+/- SEM) therefore represent interassay variation only.

Previous studies with fish and mammals indicate that myostatin expression is influenced by different stressors (Carlson et al., 1999; Gonzalez-Cadavid and Bhasin, 2004; Vianello et al., 2003; Wehling et al., 2000). Adult zebrafish were therefore subjected to 3 days of acute stocking density stress to determine changes in zfMSTN-1 and -2 gene expression in muscle, brain and spleen. Due to the dramatic difference in absolute levels and the degree of changes, transcript levels of both genes are shown as normalized expression on a logarithmic scale and as percent of control (Fig. 7). In muscle and brain transcript levels of both zfMSTN-1 and -2 did not significantly change. The greatest changes in myostatin gene expression, however, occurred in the spleen. Levels of both zfMSTN-1 and -2 mRNA increased by almost 3 log orders of magnitude over the LD levels. These dramatic increases in expression of both genes suggests that myostatin plays an important role in modulating immune system function during conditions of stress. These results together suggest that zfMSTN-1 and -2 are differently regulated by stocking density stress in a gene and tissue-specific manner. They also implicate myostatin in mediating the effects of stress on the immune system, which has never been described in any vertebrate model.

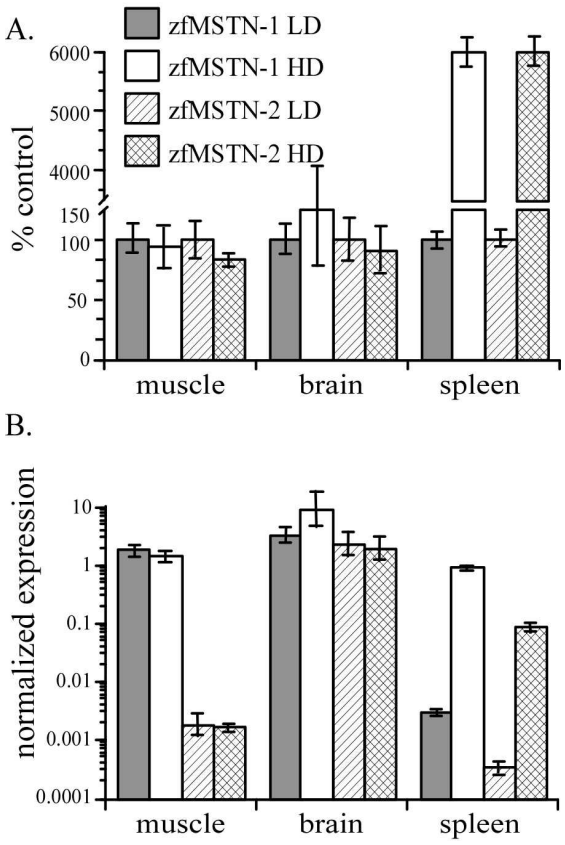

Figure 7. Stocking density stress and zebrafish myostatin expression. The effect of acute stocking density stress on the expression of zfMSTN-1 and -2 in muscle, brain and spleen was determined by qRT-PCR. High density (HD) fish were housed at a density of 40 fish/L water. Low density (LD) fish were housed at a density of 5 fish/L. Fish were housed in 3 tanks per treatment group to control for tank effect. HD and LD treatments were repeated twice. A. Relative expression levels of zfMSTN-1 and -2 were compared to percent of control. B. Mean normalized levels of zfMSTN-1 and -2 shown in logarithmic scale. Mean values shown (+/- SEM).

CHAPTER THREE

IMPLICATIONS OF NOVEL MYOSTATIN FUNCTION

Discussion

Myostatin function has been extensively studied in mammalian skeletal muscle however, its function may be quite different in fish where its expression occurs in many more adult and developing tissues. A recent phylogenetic analysis has identified two distinct myostatin clades, suggesting that all fish express at least two myostatin genes. These genes have been cloned from zebrafish and from a select few other species and relatively little is known about their expression pattern. This highlights the need for more extensive studies of MSTN-2 expression patterns during embryonic development and in adult tissues.

In this study, we characterized and quantified the expression patterns of zfMSTN-1 and -2 genes in developing zebrafish embryos and in adult tissues. High expression levels of both genes during blastula stages is indicative of remaining maternal transcripts, which was observed in other studies that measured myostatin expression in unfertilized embryos from zebrafish (Vianello et al., 2003) and from other fish species (Roberts and Goetz, 2001; Rodgers et al., 2001a), the purpose of which is to program the earliest stages of development. Both transcripts were nearly undetectable during gastrulation. This indicates that neither transcript is necessary at this stage and is consistent with previous qualitative assessments of myostatin expression in developing tilapia embryos (Rodgers et al., 2003). *In situ* hybridization studies of myostatin expression in mice determined that it is first detected in the myotome compartment of somites, which contains myogenic cells that eventually form mature skeletal muscle. As somitogenesis

progresses in mice, levels of myostatin increase, although expression is limited almost exclusively to developing skeletal muscle. In this study, expression patterns of either zfMSTN-1 or -2 do not necessarily follow the patterns of muscle development, although the changes in expression of both genes during somitogenesis are consistent with the early stages of myogenesis. Levels of zfMSTN-1 mRNA steadily rise throughout somitogenesis (21.5 hpf) and then abruptly 24 hpf while zfMSTN-2 levels peak and drops during early somitogenesis (11.3 hpf). The formation of trunk and tail somites is similarly controlled, although some of the factors that influence this process are different. This is best illustrated by comparing somite formation and MRF gene expression in spadetail (spt), one-eyed pinhead (Oep) and no-tail (ntl) mutants or in spt:Oep double mutants (Griffin and Kimelman, 2002; Weinberg et al., 1996). Paraxial mesoderm segregates in the cranial to caudal directions and results in the temporal formation of somites and in the development of the somite myotome. Therefore, the early expression of zfMSTN-2 is consistent with the onset of myogenesis in the trunk while the zfMSTN-1 expression pattern is consistent with the same extensive process that occurs in the tail. A definitive role for each myostatin during the early stages of muscle development remains unknown. Nevertheless, the expression pattern of both genes in zebrafish suggest that both are likely involved.

Analysis of mammalian skeletal muscle indicates that myostatin is limited primarily to this tissue in adults, however weak expression has also been detected in Purkinje fibers and cardiomyocytes of sheep (Sharma et al., 1999), in porcine lactating mammary glands (Ji et al., 1998) and in adipose tissue (McPherron and Lee, 2002). To date, the only known function of myostatin is to negatively inhibit skeletal muscle growth

and development, which has been indicated by numerous studies using muscle cell lines, in myostatin null mice, cattle, and in one human (Grobet et al., 1997; Kambadur et al., 1997; Lee and McPherron, 1999; McPherron et al., 1997; McPherron and Lee, 1997; Schuelke et al., 2004). Myostatin's more ubiquitous expression in various tissues of several fish species (Maccatrozzo et al., 2001a; Maccatrozzo et al., 2001b; Radaelli et al., 2003; Rescan et al., 2001; Roberts and Goetz, 2001; Rodgers and Weber, 2001; Rodgers et al., 2001a) suggests that its functions may be equally diverse. These studies have determined that myostatin is present not only in skeletal muscle, but also in eyes, brain, gill filaments, gonads and gut of tilapia (Rodgers et al., 2001a). Ostbye *et al*. (2001) additionally identified message in heart, spleen, and tongue of Atlantic salmon, while Rescan *et al.* (2001) identified it in all of these tissues of rainbow trout and in heart, kidney, and liver. Similar studies by other groups using different and diverse fish species confirm this ubiquitous expression pattern. However, these studies were performed before the discovery of two distinct myostatin gene families in fish. Thus, these previous studies may have focused on only the zfMSTN-1 or may have inadvertently sampled both transcripts simultaneously. Furthermore, none of these studies were quantitative and thus, the relative contribution of each gene product within a specific tissue is unknown. We determined both zfMSTN-1 and -2 genes are expressed in a wide variety of tissues in zebrafish as was expected. Both transcripts are present in brain, muscle, gills, eyes, skin, gastrointestinal tract, heart, spleen, liver, swim bladder, ovaries and testes. However, the levels of expression were quite different between tissues and somites between genes. The tissues with the highest expression of both genes are brain, muscle, eyes, heart, testes and surprisingly spleen.

The possibility that myostatin may have different functional roles in fish versus mammals is only just beginning to be studied. In mammals, myostatin expression increases in muscles undergoing atrophy or disease states (Baldwin, 1996; Gonzalez-Cadavid and Bhasin, 2004). In contrast, chronic crowding stress decreases myostatin expression in zebrafish skeletal muscle (Vianello et al., 2003). A similar result was observed in tilapia subjected to chronic nutritional stress (Rodgers et al., 2003) and during sexual maturation in rainbow trout, a time when muscle undergoes atrophy (Rescan et al., 2001). These studies indicate differential responses to stress in mammals as fish. Although any particular stressor can impact tissues and organisms was not shared by other stressors, hypercortisolemia commonly develops irregardless of the stressor. Glucorticoids increase myostatin gene expression in mammals (Weber et al., 2005; Wehling et al., 2000) and decrease MSTN-1 levels in tilapia larvae (Rodgers et al., 2003), which could explain the differential response to stress in mammals and fish. Overcrowding is a common problem encountered in the aquaculture industry and often results in increased incidence of disease. Myostatin's precise immune function is unknown, however, if its inhibitory role in muscle is conserved in the spleen and possible other immune tissue, the upregulation of both MSTN-1 and -2 genes could contribute to stress induced immunocomprimization.

At present, only a few studies have attempted to determine if myostatin influences skeletal muscle growth in fish and so far the results are still inconclusive. Overexpression of the myostatin prodomain or "LAP" in zebrafish resulted in a slight (10-15%) increase skeletal muscle cell number however, this was not accompanied by an increase in cell size or in the expression of the MRFs, MyoD, Myf5 and myogenin (Xu et al., 2003).

Myostatin null zebrafish have been described in two studies, although each is highly controversial and conflict with other reports. Amali *et al*. (Amali et al., 2004) reported enhanced somitogenesis, expression of the myogenic regulatory factors (MRF) MyoD and myogenin (by non-quantitative RT-PCR) and whole embryo size using morpholino "knock down" technology. These results are in stark contrast to an earlier study by Xu *et al*. (Xu et al., 2003) who generated LAP transgenic fish without a significant muscle phenotype or changes in MRF expression. Attempts by Amali *et al*. (2004) to validate the knock-down of myostatin protein were highly questionable as western blotting (using antiserum against human myostatin) identified only a single band of 27 kDa rather than the 13 kDa processed and 42 kDa unprocessed myostatin proteins previously characterized by Vianello *et al*. (Vianello et al., 2003) who used two different antisera generated specifically against zebrafish myostatin. Acosta *et al*. (Acosta et al., 2005) also claimed to have generated "giant zebrafish" by injecting double-stranded tilapia myostatin RNA into zebrafish embryos. Injections of $5x10^6$ or even just 5 molecules/embryo at the single cell stage were both reported to have increased whole animal size after 75 days. The authors made no attempt to measure myostatin protein or to explain the improbability of an effect with just 5 molecules. Most damaging to their conclusions was the fact that the controls of one experiment were actually larger than the treated of the other. The reported differences were most likely due to normal size variations within the population and not to disruption of myostatin. Both of these studies were performed before our discovery of the second class of fish myostatin genes (Kerr et al., 2005), which further complicates the interpretation of their results. Whether or not a myostatin null phenotype can be created in fish remains to be determined. However, the

presence of multiple myostatin genes and their unique expression patterns suggest that future attempts may need to target a specific gene or at least skeletal muscle expression *per se*.

APPENDIX

PROTOCOL FOR REAL-TIME RT-PCR

Real-time RT-PCR has become a widely used method for quantifying gene expression because it is highly sensitive, sequence specific and requires no post-amplification processing. In order to benefit from this assay, a clear understanding of sample processing and amplification methods is required. Therefore, this protocol was designed to help individuals learn a real-time RT-PCR technique using the SYBR I green reporting system.

Guidelines for proper primer design for SYBR green I assays.

As SYBR green I binds to any dsDNA it is important to avoid primer-dimers and/or non-specific products. By selecting amplicons between 80 and 150 bp a high level of fluorescence can be obtained without compromising the PCR efficiency.

Primer Guidelines

- Use software such as PrimerExpress® to create primers
- Each primer should be between 18-30 bases
- GC content 30-80% (ideally 40-60%)
- Tm 63-67°C (ideally 64°C) so that annealing is 58-62°C. ΔTm should be< 4°C.
- Avoid mismatches between primers and target, especially at 3' end of the primer
- Avoid runs of identical nucleotides, especially of 3 or more G's or C's at the 3' end.
- Avoid 3' end T (allows mismatching)
- Avoid complementarity within the primers to avoid hairpins
- Avoid complementarity between primers, especially at 3' end to avoid primer dimer
- Design intron spanning primers to prevent or identify the amplification of contaminating gDNA. For intron spanning primers the first half of the oligo must

hybridize with the 3' end of one exon and to the 5' end of the other exon. In this way only cDNA will be amplified and gDNA not. For intron flanking primers the forward primer must hybridize to one exon and the reverse primer to the other exon. Amplicon length should then be 80-150 bp. Amplicons from cDNA, without intron, will be smaller than amplicons from gDNA, which will contain the intron. The difference in size of these amplicons can be determined by melt curve analysis and by analysis with a DNA gel by measuring amplicon size. Genomic DNA can be avoided by DNase treatment of the RNA with RNase free DNase.

Amplicon

- Length 80-150 bp
- Shorter amplicons will give higher efficiencies
- Longer amplicons will give higher ΔRn as more SYBR green I is incorporated
- Avoid secondary structures in the amplicon (check Mfold www.bioinfo.rpi.edu/applications/mfold/).

TRIzol (Invitrogen, invitrogen.com) RNA isolation protocol

(Do all TRIzol work in a chemical fume hood as TRIzol contains acidic phenol and is extremely corrosive to the skin and can cause headaches)

1. Freeze tissue immediately after obtaining in liquid N_2.
2. Weigh frozen tissue and use ~50-100 mg per ml of TRIzol.
3. Put tissue in vial and add TRIzol and homogenize until all visible tissue is gone.
4. Incubate at RT for 5 min to dissolve nucleoproteins.
5. Add 200 µl chloroform per ml TRIzol, vortex and incubate at RT for 2 min.
6. Centrifuge sample at 12K x g for 15 min at 4°C.

7. Remove upper clear aqueous layer, which contains RNA and transfer to new tube. Be careful not to touch the organic layer with pipet tip as this will increase gDNA contamination. Discard the organic and inner phases in phenol waste.

8. Add equal amount of isopropanol to the aqueous phase, vortex and incubate at RT for 10 min to precipitate RNA. Higher yields can be obtained by incubating at 20°C for 15-60 min.

9. Centrifuge at 12K x g for 15 min at 4°C.

10. Remove the supernatant first by pouring with the pellet facing you.

Concentrate the remaining supernatant with a quick spin and remove with a hydrophilic aerosol barrier RNase free gel loading tip.

11. Wash the pellet once by vortexing in ice cold 75% EtOH (in DEPC-H20). The volume of EtOH should be greater than or equal to the initial TRIzol volume.

12. Centrifuge at 7.5K x g for 5 min at 4°C and remove supernatant. Allow to air dry (~5 min) at RT, dissolve in 20 µl DEPC-H2O. If the pellet is too dry and does not dissolve, add ~20 µl 1% SDS and incubate at 50°C for 10 min.

13. Quantify RNA using a spectrophotometer

Note: it is recommended to treat RNA with DNase to remove any contaminating gDNA.

DNA free (Ambion, ambion.com) DNase Treatment protocol

1. Transfer RNA to 0.5 ml tube.

(Add 0.1 volume 10X buffer and 1µl rDNase I per 10 µg RNA)

For 50 µl reaction add:

5 µl DNaseI buffer

X µl RNA

1 µl rDNase per 10 µg RNA

QS to 50 µl with DEPC-H2O

Mix gently, incubate at 37°C for 30 min

2. Vortex DNase Inactivation reagent to mix well and add 5 µl to DNase treated RNA mixture. Incubate at RT for 2 min, mixing by pipetting up and down 2-3 times to redisperse the DNase Inactivation Reagent.

3. Centrifuge at 10K x g for 1.5 min.

4. Transfer supernatant containing RNA to new tube, follow precipitation protocol or store at -80°C.

Precipitation of RNA protocol

1. To RNA add 0.1 volume molecular grade 3M sodium acetate pH 5.2

2. Add 3 volumes of ice cold 100% EtOH

3. Centrifuge at 10K x g for 1.5 min

4. Remove supernatant and wash pellet 2X with 100 µl of 70% ice cold EtOH, centrifuging.

5. Quantify RNA

Make cDNA from RNA using First Strand DNA synthesis protocol from Invitrogen. Superscript (SS) III reverse transcriptase will produce higher quantities of RNA, however SS II reverse transcriptase is acceptable. Omit DTT from cDNA protocol. DTT normally protects disulfide bonds from oxidation, however SYBR green is a minor groove binding dye, therefore DTT may inhibit binding of SYBR green during the qPCR reaction and will not give good results (Deprez, 2002). For qRT-PCR of a gene that is of low transcript level, use between 1 and 5 µg RNA to make cDNA.

First-Strand cDNA Synthesis Using SuperScript™ III for RT-PCR

1. Add the following components to a nuclease-free microcentrifuge tube:

1 µl of 50 µM (or 200-500 ng) of oligo$(dT)_{18}$.

1 to 5 µg of RNA

1 µl of 10 mM dNTP mix

QS to 13 µl with sterile nuclease-free water

2. Heat mixture to 65°C for 5 min and incubate on ice for at least 1 min.

3. Collect the contents of the tube by brief centrifugation and add:

4 µl 5X First-Strand Buffer

1 µl RNaseOUT™ Recombinant RNase Inhibitor. Note: When using less than 50 ng of starting RNA, the addition of RNasOUT™ is essential.

1 µl of SuperScript™ III RT (200 units/µl)

4. Mix by pipetting gently up and down. If using random primers, incubate tube at 25°C for 5 min.

5. Incubate at 50°C for 30-60 min. Increase reaction temperature to 55°C for gene-specific primer. Reaction temperature may also be increased to 55°C for difficult templates or templates with high secondary structure.

6. Inactivate the reaction by heating at 70°C for 15 min.

The cDNA can now be used as a template for amplification in qPCR.

Recommendations for Optimal Results

Due to the sensitivity of qRT-PCR, results can be easily affected by pipetting errors.

- Always prepare a master mix of iQ SYBR Green Supermix containing the primers and probe.

- Add the template DNA sample to aliquots of the master mix for optimal reproducibility of replicate samples.

- This allows you to pipet once into the sample well or tube. Individual pipetting of replicate samples is not recommended.

Protocol for qRT-PCR setup

**If using iCyler thermocycle machine, turn on and let warm for at least 15 minutes before using.

1. To make master mix of qRT-PCR reagents, first vortex and mix IQ SYBR green well before using.

For 25 µl reaction volume add	IQ SYBR green	12.5 µl
	Primer F	1 µl
	Primer R	1 µl
	H_2O	9.5 µl
	cDNA	1 to 1.5 µl

Note: Keep all reagents on ice while making master mix.

2. Aliquot master mix into Real-Time RT-PCR 96-well Thin Wall plates (USA Scientific, usascientific.com) being careful not to create bubbles in wells, and take to iCycler thermocycler machine. Place 96-well plate wells of reader plate, remove backing of qRT-PCR sealing tape and without touching any part of the sealing tape except the edges, apply the sealing tape to plate. Seal tape on plate with flat plastic wedge going in one

direction horizontally and one direction vertically. Once tape is sealed on plate, close machine.

3. Enter your user name in iCycler machine.

4. Open iCycler program in computer, and create thermal protocol by clicking "Create a new protocol". The Edit Protocol window of the Workshop module will open.

5. Start in the spreadsheet at the bottom left of the window and fill in the thermal cycling protocol. As you make changes in the spreadsheet, they are reflected in the graphical representation at the top of the window. The cycle being edited is shown in blue on the bar across the top of the graph and is highlighted in blue in the spreadsheet.

- Double click in a time or temperature field to change the default settings.

- Insert a new cycle in front of the current cycle by clicking "Insert Cycle" and then clicking anywhere on the current cycle in the spreadsheet. Insert a cycle after the last cycle by clicking "Insert Cycle" and then clicking anywhere on the first blank line at the bottom of the spreadsheet. If you right mouse click on the "Insert Cycle" button, you can choose to insert a 1, 2 or 3-step cycle. When finished, deselect "Insert Cycle".

- Delete cycles by clicking "Delete Cycle" and then clicking anywhere on that cycle in the spreadsheet. When finished, deselect "Delete Cycle".

- Insert a step in front of the current step by clicking "Insert Step" and then clicking on the current step. If you right mouse click on the "Insert Step" button, you can choose to insert the new step before or after the current step. When finished, deselect "Insert Step".

- Delete steps by clicking "Delete Step" and then clicking anywhere on the line containing the step to be deleted. When finished, deselect "Delete Step".

7. If you want to add any protocol options, first enable them by clicking in the check box next to its description in the Show options box.

- Infinite Hold. A column labeled Hold will appear in the spreadsheet. Click the Hold button on any step of a non-repeated cycle and the set point temperature will be maitained indefinitely until user intervention. A red check mark will appear in the Hold column of the spreadsheet. Turn off the Hold by clicking on the red check mark. The software will not allow you to program a Hold if the cycle is repeated.

- Gradient. Two new columns appear in the spreadsheet. Click the Gradient button on the desired step. Specify the range of the gradient in the other column. The range may be from 1° to 25°C across the block and the block temperatures must be in the range of 40° to 95°C.

- Melt Curve. Three new columns appear in the spreadsheet. Click the Melt Curve column on the step at which melt curve data are to be collected. Indicate the temperature increment or decrement with each cycle. A green camera will appear on the corresponding step in the Select Data Collection Step box.

- Increment Temperature/Decrement Temperature. Three new columns will appear. Specify the increment or decrement in temperature, the first cycle at which the change is to occur and the frequency with which the change is to occur. For example, to increase temperature by 0.2°C beginning with the third cycle and to further increase the temperature every other cycle after that you would enter 0.2 in the + Temp column, 3 in the Begin Repeat column and 2 in the How Often column.

- Ramping. Double click in the Ramping column and choose MIN or MAX or make a direct entry of heating or cooling rate. Valid entries are from 0.1° to 3.3°C/sec for heating steps and 0.1° to 2.0°C/sec for cooling steps.

- Cycle Description/Step Process. One new column appears if either of these is selected. Choose a descriptive name from the pull down menu or enter one directly.

8. In the "Select data collection steps" box, specify the cycles at which fluorescent data are to be collected for quantitative experiments.

- Click once in a camera square to indicate that data are to be collected for post-run analysis. A camera with a yellow lens will appear in the box and on the graphical display.

- Click a second time to indicate that fluorescent data are to be collected and analyzed in real time. REAL TIME will appear next to the yellow camera in the Select data collection step box.

- Click a third time to deselect data collection for that cycle. The camera icon will disappear.

9. Double click in the Protocol Fine Name text box and enter a new name for the protocol.

10. Click "Save this protocol". A Save dialog box will appear, click Save again, Creating a New Plate Setup in Whole Plate Mode

11. From the Library, select the "View Plate Setup" tab

12. Click "Create new plate setup". The Edit Plate Setup window of the Workshop module will open.

13. Icon Functions

The toolbar menu contains the following icons that may be used to identify the types of samples in each well of the Plate Layout.

Icon Description

Cursor Used to select a specific well in the Plate Layout.

Standard Used to identify wells that contain known amounts of the template being assayed. Wells in the Plate Layout identified as standards are given sequential numbers when they are selected. Replicate wells containing the same concentrations of standards are labeled with the same number (see Section 5.2.3.4.) The Define Standards box on the right side of the Edit Plate Setup window is active when the Standard icon is active and a well containing the standard is selected; the concentration of the template in each of the Standards must be specified in the Quantity text box and the units of measure are specified from the Units list box (see Section 5.2.3.3).

Unknown Used to identify wells that contain samples with an unknown quantity of the template being assayed. Wells in the Plate Layout identified as unknowns are given sequential numbers when they are selected; replicate wells containing the same amount of template are indicated by the same number (see Section 5.2.3.4.)

Blank Used to identify wells without any reaction mixture.

+Control This icon allows you to identify wells with a sample containing the compound of interest; in Endpoint Assays, this is useful to define the range of the results. Use this icon to identify homozygous controls

in allelic discrimination assays.

-Control Used to identify wells that contain samples missing one or more of the parts of the reaction mixture; in Endpoint Assays, this is useful to define the range of the results. Use this icon to identify no-template controls in allelic discrimination assays.

Pure Dye Used to identify wells containing pure fluorophore for pure dye calibration protocols.

Erase Used to clear identification from previously specified wells.

Fluorophore specification is also erased.

Click on appropriate icon, then click in appropriate well to specify well, then enter sample well description into sample well area.

14. Once all wells have been defined, click "Select and Load Fluorphores" tab and look in the Fluorophore Pallette box.

15. Choose one of the filter wheel setups available from the pull down menu, a set of fluorophores will be displayed in the Fluorophore Selection box.

Note: at this time click FAM-490 as this is the only filter available.

Click the box next to the desired fluorophore in the Fluorophore Selection box

16. Click on a crayon in the Fluorophore Pallette box to associate the fluorophore with a color.

Note: at this time click on the green crayon.

17. Click on each well to be monitored for that fluorophore.

18. Click "Save this plate setup"

19. To start an experiment with the currently selected protocol file, click "Run with selected protocol".

20. Enter the reaction volume in the sample volume box, and click "Begin Run".

Note: when reaction is finished iCycler automatically saves data in Library module.

View post-run data

21. When the qRT-PCR run cycles are finished click "View Post Run Data"

22. You may choose which window to view data.

If you choose PCR Quantification tab the analysis curve and Ct cycles will be shown.

In the Select Analysis Mode, select Baseline Subtraction Curve Fit for best results.

23. Click "Reports" for a file that lists all post run data for analysis. This file must be saved to another folder and then may be printed.

For further information on the many different analysis tools available with the iCycler program refer to iCycler iQ™ Real-Time PCR Detection System Instruction Manual Available from the BioRad website catalog number 170-8740.

For optimal results for qRT-PCR there are many different parameters of the assay which may need to be optimized.

1. Find the optimal denaturation time, annealing temperature and time, and extension time for your particular assay.

2. Primer concentration must be optimized for each primer combination. By doing this type of optimization it is also possible to compensate for differences up to 2°C in Tm of the primers. A helpful matrix for finding the optimal primer concentrations is as follows:

Table 2. Matrix for primer optimization.

	Reverse				
Forward	900 nM	600 nM	300 nM	150 nM	50 nM
900 nM	900/900	900/600	900/300	900/150	900/50
600 nM	600/900	600/600	600/300	600/150	600/50
300 nM	300/900	300/600	300/300	300/150	300/50
150 nM	150/900	150/600	150/300	150/150	150/50
50 nM	50/900	50/600	50/300	50/150	50/50

Refer to Eurogentec.com and look up qPCR troubleshooting guide for other helpful suggestions.

3. $MgCl_2$ concentrations also may be too high or too low. Adjust in concentrations of 0.5 mM steps.

4. If you have high fluorescence in No Template Control or No Reverse Transcriptase Control there is possible contamination with genomic DNA. Treat RNA with DNase and make sure primers are designed properly.

5. If more than one peak is visible in the Melt Curve then there is also possible gDNA contamination. Properly designed primers and treatment of RNA with DNase should take care of this.

6. If fluorescent peak is low, try increasing the amount of starting template if template copy is low. If template copy is high, try diluting template 1:5 with water and adding 1.5 µl of template to reaction mixture. It is possible to inhibit the reaction with too much template.

Quantification Analysis Tool

A useful program for determining relative gene expression patterns is the Q-Gene program developed with Microsoft® Excel® based software (Muller et al., 2002).

CHAPTER FOUR

REFERENCES

Acosta, J., Y. Carpio, I. Borroto, O. Gonzalez, and M. P. Estrada. 2005. Myostatin gene silenced by RNAi show a zebrafish giant phenotype. J Biotechnol 119: 324-331.

Amali, A. A. et al. 2004. Up-regulation of muscle-specific transcription factors during embryonic somitogenesis of zebrafish (*danio rerio*) by knock-down of myostatin-1. Dev Dyn 229: 847-856.

Arnold, H. H., and T. Braun. 1996. Targeted inactivation of myogenic factor genes reveals their role during mouse myogenesis: A review. Int J Dev Biol 40: 345-353.

Arthur, P. F. 1995. Double muscling in cattle: A review. Aust. J. Agric. Res. 46: 1493-1515.

Baldwin, K. M. 1996. Effect of spaceflight on the functional, biochemical, and metabolic properties of skeletal muscle. Med Sci Sports Exerc 28: 983-987.

Bern, H. A., Madsen, S.S. 1992. A selective survey of the endocrine system of rainbow trout (*ochorhynchus mykiss*) with emphesis on the hormonal regulation of the ion balance. Aquaculture 100: 237-262.

Carlson, C. J., F. W. Booth, and S. E. Gordon. 1999. Skeletal muscle myostatin mRNA expression is fiber-type specific and increases during hindlimb unloading. Am J Physiol 277: R601-606.

Deprez, R. H. L., Fijnvandraat, A.C., Ruijter, Moorman, A.F.M. 2002. Sensitivity and accuracy of quantitative real-time polymerase chain reaction using SYBR green I depends on cDNA synthesis conditions. Analytical Biochemistry 307: 63-69.

Evans, R. M. 1988. The steroid and thyroid hormone receptor superfamily. Science 240: 889-895.

Gonzalez-Cadavid, N. F., and S. Bhasin. 2004. Role of myostatin in metabolism. Curr Opin Clin Nutr Metab Care 7: 451-457.

Griffin, K. J., and D. Kimelman. 2002. One-eyed pinhead and spadetail are essential for heart and somite formation. Nat Cell Biol 4: 821-825.

Grobet, L. et al. 1997. A deletion in the bovine myostatin gene causes the double-muscled phenotype in cattle. Nat Genet 17: 71-74.

Ji, S. et al. 1998. Myostatin expression in porcine tissues: Tissue specificity and developmental and postnatal regulation. Am J Physiol 275: R1265-1273.

Joulia, D. et al. 2003. Mechanisms involved in the inhibition of myoblast proliferation and differentiation by myostatin. Exp Cell Res 286: 263-275.

Kambadur, R., M. Sharma, T. P. Smith, and J. J. Bass. 1997. Mutations in myostatin (GDF8) in double-muscled belgian blue and piedmontese cattle. Genome Res 7: 910-916.

Ken, C. F., C. T. Lin, J. L. Wu, and J. F. Shaw. 2000. Cloning and expression of a cDNA coding for catalase from zebrafish (*danio rerio*). J Agric Food Chem 48: 2092-2096.

Kerr, T., E. H. Roalson, and B. D. Rodgers. 2005. Phylogenetic analysis of the myostatin gene sub-family and the differential expression of a novel member in zebrafish. Evol Dev 7: 390-400.

Kocabas, A. M., H. Kucuktas, R. A. Dunham, and Z. Liu. 2002. Molecular characterization and differential expression of the myostatin gene in channel catfish (*ictalurus punctatus*). Biochim Biophys Acta 1575: 99-107.

Langley, B. et al. 2002. Myostatin inhibits myoblast differentiation by down-regulating myod expression. J Biol Chem 277: 49831-49840.

Lee, S. J. 2004. Regulation of muscle mass by myostatin. Annu Rev Cell Dev Biol 20: 61-86.

Lee, S. J., and A. C. McPherron. 1999. Myostatin and the control of skeletal muscle mass. Curr Opin Genet Dev 9: 604-607.

Lee, S. J., and A. C. McPherron. 2001a. Regulation of myostatin activity and muscle growth. Proc Natl Acad Sci U S A 98: 9306-9311.

Maccatrozzo, L., L. Bargelloni, B. Cardazzo, G. Rizzo, and T. Patarnello. 2001a. A novel second myostatin gene is present in teleost fish. FEBS Lett 509: 36-40.

Maccatrozzo, L., L. Bargelloni, G. Radaelli, F. Mascarello, and T. Patarnello. 2001b. Characterization of the myostatin gene in the gilthead seabream (*sparus aurata*): Sequence, genomic structure, and expression pattern. Mar Biotechnol (NY) 3: 224-230.

McPherron, A. C., A. M. Lawler, and S. J. Lee. 1997. Regulation of skeletal muscle mass in mice by a new TGF-beta superfamily member. Nature 387: 83-90.

McPherron, A. C., and S. J. Lee. 1997. Double muscling in cattle due to mutations in the myostatin gene. Proc Natl Acad Sci U S A 94: 12457-12461.

McPherron, A. C., and S. J. Lee. 2002. Suppression of body fat accumulation in myostatin-deficient mice. J Clin Invest 109: 595-601.

Megeney, L. A., and M. A. Rudnicki. 1995. Determination versus differentiation and the MyoD family of transcription factors. Biochem Cell Biol 73: 723-732.

Molkentin, J. D., and E. N. Olson. 1996. Defining the regulatory networks for muscle development. Curr Opin Genet Dev 6: 445-453.

Mommsen, T. P., Vijayan, M.M. and Moon, T.W. 1999. Cortisol in teleosts: Dynamics, mechanisms of action, and metabolic regulation. Reviews in Fish Biology and Fisheries 9: 211-268.

Muller, P. Y., H. Janovjak, A. R. Miserez, and Z. Dobbie. 2002. Processing of gene expression data generated by quantitative real-time RT-PCR. Biotechniques 32: 1372-1374, 1376, 1378-1379.

Ostbye, T. K. et al. 2001. The two myostatin genes of Atlantic salmon (*salmo salar*) are expressed in a variety of tissues. Eur J Biochem 268: 5249-5257.

Radaelli, G., A. Rowlerson, F. Mascarello, M. Patruno, and B. Funkenstein. 2003. Myostatin precursor is present in several tissues in teleost fish: A comparative immunolocalization study. Cell Tissue Res 311: 239-250.

Rescan, P. Y., I. Jutel, and C. Ralliere. 2001. Two myostatin genes are differentially expressed in myotomal muscles of the trout (*oncorhynchus mykiss*). J Exp Biol 204: 3523-3529.

Rios, R., I. Carneiro, V. M. Arce, and J. Devesa. 2001a. Myostatin regulates cell survival during C2C12 myogenesis. Biochem Biophys Res Commun 280: 561-566.

Rios, R., I. Carneiro, V. M. Arce, and J. Devesa. 2002. Myostatin is an inhibitor of myogenic differentiation. Am J Physiol Cell Physiol 282: C993-999.

Roberts, S. B., and F. W. Goetz. 2001. Differential skeletal muscle expression of myostatin across teleost species, and the isolation of multiple myostatin isoforms. FEBS Lett 491: 212-216.
Roberts, S. B., and F. W. Goetz. 2003. Myostatin protein and rna transcript levels in adult and developing brook trout. Mol Cell Endocrinol 210: 9-20.
Rodgers, B. D., and G. M. Weber. 2001. Sequence conservation among fish myostatin orthologues and the characterization of two additional cDNA clones from *morone saxatilis* and *morone americana*. Comp Biochem Physiol B Biochem Mol Biol 129: 597-603.
Rodgers, B. D., G. M. Weber, K. M. Kelley, and M. A. Levine. 2003. Prolonged fasting and cortisol reduce myostatin mRNA levels in tilapia larvae; short-term fasting elevates. Am J Physiol Regul Integr Comp Physiol 284: R1277-1286.
Rodgers, B. D., G. M. Weber, C. V. Sullivan, and M. A. Levine. 2001a. Isolation and characterization of myostatin complementary deoxyribonucleic acid clones from two commercially important fish: *Oreochromis mossambicus* and *morone chrysops*. Endocrinology 142: 1412-1418.
Rudnicki, M. A., and R. Jaenisch. 1995. The MyoD family of transcription factors and skeletal myogenesis. Bioessays 17: 203-209.
Saharinen, J., M. Hyytiainen, J. Taipale, and J. Keski-Oja. 1999. Latent transforming growth factor-beta binding proteins (ltbps)-- structural extracellular matrix proteins for targeting TGF-beta action. Cytokine Growth Factor Rev 10: 99-117.
Schuelke, M. et al. 2004. Myostatin mutation associated with gross muscle hypertrophy in a child. N Engl J Med 350: 2682-2688.
Sharma, M. et al. 1999. Myostatin, a transforming growth factor-beta superfamily member, is expressed in heart muscle and is upregulated in cardiomyocytes after infarct. J Cell Physiol 180: 1-9.
Taylor, W. E. et al. 2001. Myostatin inhibits cell proliferation and protein synthesis in c(2)c(12) muscle cells. Am J Physiol Endocrinol Metab 280: E221-E228.
Thomas, M. et al. 2000a. Myostatin, a negative regulator of muscle growth, functions by inhibiting myoblast proliferation. J Biol Chem 275: 40235-40243.
Thomas, M. et al. 2000b. Myostatin, a negative regulator of muscle growth, functions by inhibiting myoblast proliferation. J Biol Chem 275: 40235-40243.
Valdez, M. R., J. A. Richardson, W. H. Klein, and E. N. Olson. 2000. Failure of Myf5 to support myogenic differentiation without myogenin, MyoD, and Mrf4. Dev Biol 219: 287-298.
Vianello, S., L. Brazzoduro, L. Dalla Valle, P. Belvedere, and L. Colombo. 2003. Myostatin expression during development and chronic stress in zebrafish (*danio rerio*). J Endocrinol 176: 47-59.
Weber, T. E., B. C. Small, and B. G. Bosworth. 2005. Lipopolysaccharide regulates myostatin and myod independently of an increase in plasma cortisol in channel catfish (*ictalurus punctatus*). Domest Anim Endocrinol 28: 64-73.
Wehling, M., B. Cai, and J. G. Tidball. 2000. Modulation of myostatin expression during modified muscle use. Faseb J 14: 103-110.
Weinberg, E. S. et al. 1996. Developmental regulation of zebrafish MyoD in wild-type, no tail and spadetail embryos. Development 122: 271-280.
Wendelaar Bonga, S. E. 1997. The stress response in fish. Physiol Rev 77: 591-625.

Xu, C., G. Wu, Y. Zohar, and S. J. Du. 2003. Analysis of myostatin gene structure, expression and function in zebrafish. J Exp Biol 206: 4067-4079.
Zapf, J., and E. R. Froesch. 1999. Insulin-like growth factor-I actions on somatic growth. In: J. L. Kostyo and H. M. Goodman (eds.) Handbook of physiology, the endocrine system: Hormonal control of growth No. V. p 663-700. Oxford University Press, New York.
Zimmers, T. A. et al. 2002. Induction of cachexia in mice by systemically administered myostatin. Science 296: 1486-1488.